

Mechanical Anisotropy of Aluminium Laminates Produced by ARB

P. Chekhonin^{1,a}, B. Beausir^{1,b}, J. Scharnweber^{1,c}, C.-G. Oertel^{1,d},
J. Jaschinski^{2,e}, T. Hausöl^{3,f}, H.W. Höppel^{3,g}, H.-G. Brokmeier^{4,h}
and W. Skrotzki^{1,i}

¹ Institut für Strukturphysik, Technische Universität Dresden, D-01062 Dresden, Germany

² Institut für Leichtbau und Kunststofftechnik, Technische Universität Dresden,
D-01062 Dresden, Germany

³ Lehrstuhl Allgemeine Werkstoffwissenschaften, Universität Erlangen-Nürnberg,
D-91058 Erlangen, Germany

⁴ Helmholtz-Zentrum Geesthacht, D-21494 Geesthacht, Germany

^apaul.chekhonin@mailbox.tu-dresden.de, ^bbeausir@physik.phy.tu-dresden.de,

^cj.scharnweber@physik.tu-dresden.de, ^doertel@physik.tu-dresden.de,

^ejoern.jaschinski@ilk.mw.tu-dresden.de, ^ftina.hausoel@ww.uni-erlangen.de,

^ghoepfel@ww.uni-erlangen.de, ^hheinz-guenter.brokmeier@hzg.de,

ⁱwerner.skrotzki@physik.tu-dresden.de

Keywords: Aluminium Laminates, Accumulative Roll Bonding (ARB), Texture, Mechanical Anisotropy, Lankford Parameter

Abstract.

The plastic anisotropy was studied on aluminium sheets with layers of different purity (A: 5N and B: 2N+) produced by accumulative roll bonding (ARB). Both material layers show a contrasting recrystallization behavior where A and B are discontinuously and continuously recrystallized, respectively. Global textures were measured by neutron diffraction. The mechanical anisotropy was measured by tensile testing after different numbers of ARB cycles. The planar anisotropy decreases with the number of ARB cycles while the normal anisotropy reaches a plateau after 4 cycles. Simulations of the Lankford parameters were carried out with the help of the viscoplastic self-consistent scheme (based on the global texture) and compared with the experimental data. Deviations of the simulated values from those of experiment are discussed with regard to through-thickness texture and material heterogeneities.

Introduction

Bulk ultrafine-grained (UFG) materials produced by accumulative roll bonding (for processing details see [1,2]) have very interesting mechanical properties [3] mainly because of a significant grain refinement (grain sizes smaller than 1 μ m). In contrast to conventional rolling due to repeated stacking and roll bonding shear strain is inserted into the material. Moreover, ARB has the potential for producing composites by applying ARB to sheets of different materials or ready-prepared sandwiches [4]. Because of its simplicity this process also has a high potential for industrial applications.

During deep drawing of sheets there are unwanted effects of wall thinning and earing. These effects are influenced by the texture and can be quantified with the help of the Lankford parameter. Previously [5], the anisotropy of aluminium sheets produced by ARB had been measured and simulated. In the present work, the sheets contain through-thickness deformation-induced heterogeneities due to the ARB process itself and additional heterogeneities of materials and microstructures. The limits of the information given by the global texture measurements are tested and discussed by using the viscoplastic self-consistent polycrystal model to simulate the Lankford parameters.

Experimental Details

Aluminium sheets of high (99.999 wt% Al – labelled as A) and commercial (99.5 wt% Al – labelled as B) purity were annealed for 1 hour at 500°C. ARB was applied using a four-high rolling mill (Carl Wezel, Mühlacker, roll diameter = 32 mm) after wire brushing. The processing was performed up to 8 ARB cycles at ambient temperature without lubrication. For every cycle the orientation of the sheet halves was maintained, resulting in an asymmetric through-thickness distribution – AB after one cycle, ABAB after two cycles etc. The microstructure was observed with a Zeiss Ultra 55 scanning electron microscope. The global texture of the initial materials (A and B) and all laminates was measured by neutron diffraction (GKSS Research Center Geesthacht, Germany) on cubes of stacked ARB sheets with dimensions of (10 mm × 10 mm × 10 mm). From the measured (111), (200) and (220) pole figures the orientation distribution function (ODF) was calculated with the software Labotex (Labosoft s.c.) using the Arbitrary Defined Cells method. Tensile tests were performed with a Roell/Zwick 250 deformation machine at ambient temperature with a strain rate of $9.2 \times 10^{-4} \text{ s}^{-1}$. The tensile specimens with a gauge section of 35 mm were produced by spark erosion. The Lankford parameter r_α was measured for 3 different directions (angle between tensile direction and rolling direction $\alpha \in \{0^\circ; 45^\circ; 90^\circ\}$, referring to as r_{RD} , r_{45° and r_{TD} , RD = rolling direction, TD = transverse direction). For all cycles and each direction at least 3 measurements were done. The strain was measured with the optical system Aramis (GOM mbH, Germany) yielding the elongation $d\varepsilon_x$ and the width reduction $d\varepsilon_y$ simultaneously. Assuming volume constancy the Lankford parameter r_α is given by:

$$r_\alpha = -\frac{d\varepsilon_y}{d\varepsilon_x + d\varepsilon_y}. \quad (1)$$

The normal anisotropy $\langle r \rangle$ and its variation Δr , the planar anisotropy, are calculated by

$$\langle r \rangle = (r_{RD} + r_{TD} + 2r_{45})/4 \quad \text{and} \quad (2)$$

$$\Delta r = (r_{RD} + r_{TD} - 2r_{45})/2. \quad (3)$$

The measured Lankford parameter depends on strain, i.e. not reaching a constant value after a certain strain for most of the tensile tests. Therefore, the value at half of the fracture strain was used. All data given for the initial material B are taken from [5].

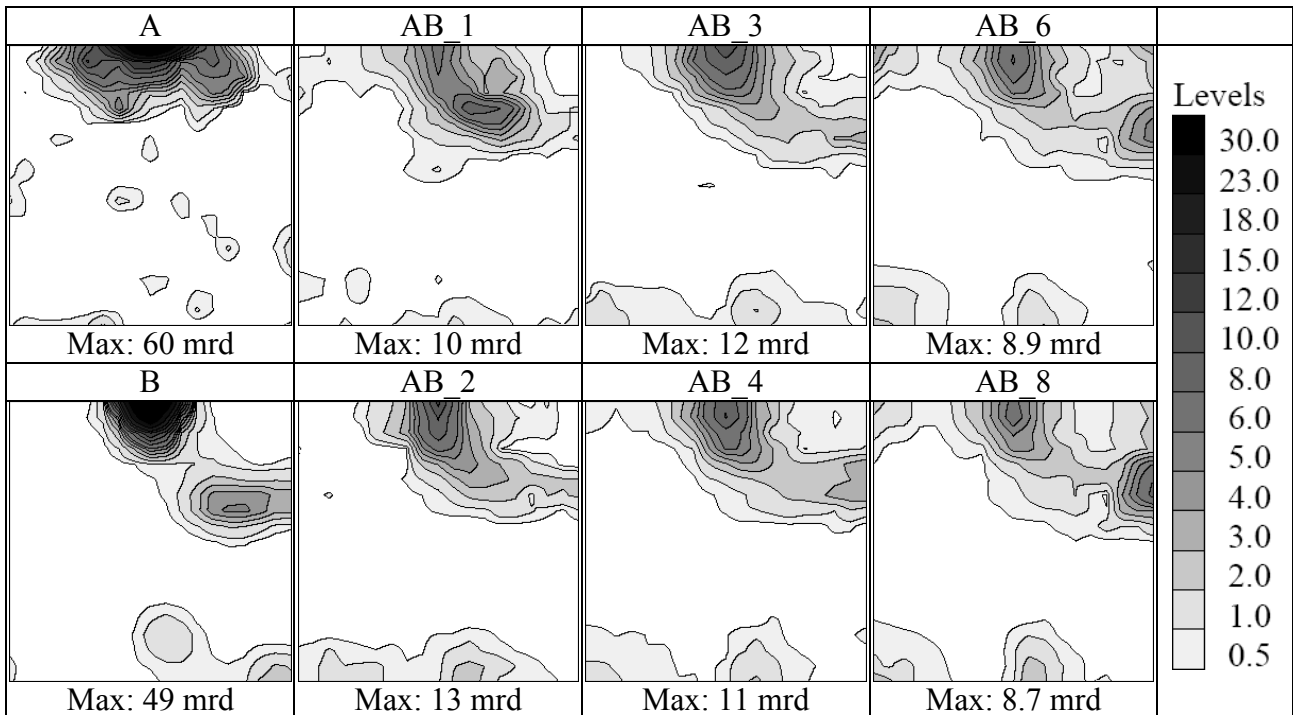
With 10,000 discrete orientations exported from the global texture, the Lankford parameter was simulated with the viscoplastic polycrystal self-consistent model [6]. Three values of the strain rate sensitivity index $m \in \{0.05; 0.1; 0.2\}$, and possible non-octahedral slip by the index $p \in \{1.00; 1.25; 1.50; 1.73\}$ were tested, with p being the ratio of reference stresses for non-octahedral and octahedral slip, for more details see [5].

Results and Discussion

The global textures of the initial materials and the laminates after different ARB cycles are presented by $\varphi_2 = 45^\circ$ ODF sections (Fig. 1a). Fig. 1b shows the corresponding positions of the main texture components. The initial materials display a very strong cube recrystallization texture. Additionally, in B some remnants of Copper (Cu), Brass (Bs) and Goss (G) rolling orientations are present.

After ARB the texture changes to a mixture of a typical rolling texture of face-centred cubic (fcc) metals, consisting of Cu, Dillamore (D), Bs and S orientations (S can be observed in the $\varphi_2 = 65^\circ$ ODF section) and the typical cube recrystallization plus a rotated Goss (RG) component. After 6 ARB cycles a noteworthy rotated Cube (C) component appears in the global texture. The C component is a shear texture component, which develops in the surface layer of rolled sheets due to friction with the rolls [7]. Unusual is the appearance of the Cube and RG components after large

accumulated strains. To explain this, one has to take a look on the microstructure of the laminate (Fig. 2). With increasing number of ARB cycles an ultrafine-grained structure develops in the B layers by continuous recrystallization [8], while discontinuous recrystallization occurs in the A layers.



a)

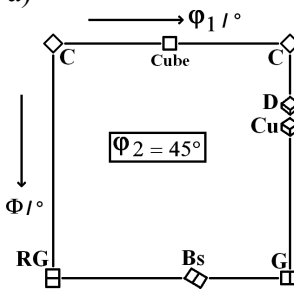


Fig 1:

(a) Textures of the initial materials and the laminate after different number of ARB cycles. The laminates are labelled as AB_#, with # being the number of ARB cycles.

(b) Key figure of the main texture components of rolled fcc metals presented by the $\phi_2 = 45^\circ$ ODF section.

b)

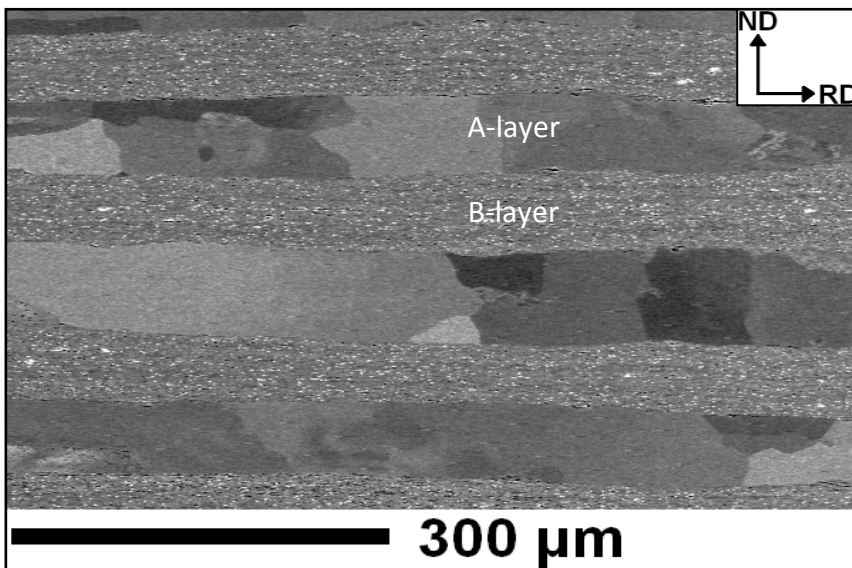


Fig. 2: Structure of the AB laminate after 4 ARB cycles.

After about three to four ARB cycles, the size of the recrystallized grains in the A layers is about the thickness of the layers. Thus, the recrystallization is limited in the normal direction (ND) leading to recrystallized grains elongated in RD and TD. A comparable microstructure was previously observed in [9], where a laminate of commercial purity aluminium and an aluminium alloy containing Sc was produced by ARB.

However, in [9] discontinuous recrystallization of the layers with higher purity was only achieved by heat treatment after ARB, whereas in the present work this structure is achieved by ARB processing at ambient temperature (an estimate of the elevated temperature due to adiabatic heating during the ARB process is about 70°C).

Recrystallization of aluminium of very high purity at ambient temperature was already observed earlier [10]. This behavior is simply explained by the reduced pinning of grain boundaries in the high purity layers, leading to high grain boundary mobility, so that recrystallization can occur at (comparatively) low temperatures and small driving forces, despite the high stacking fault energy of aluminium. As the cube component is typical for recrystallization of fcc metals [11], its appearance in the global texture, even after large accumulated strains is understandable.

The measured and simulated Lankford parameters are plotted in Fig. 3 and Fig. 4, respectively.

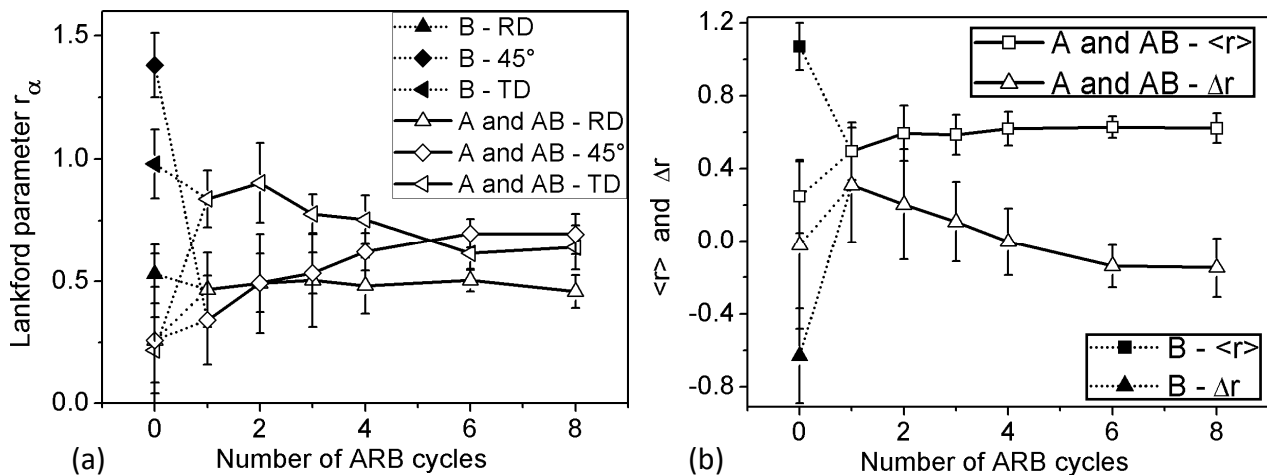


Fig. 3: (a) Measured Lankford parameter r_α , (b) normal ($\langle r \rangle$) and planar (Δr) anisotropy as a function of the number of ARB cycles. The starting materials A and B are connected to the composite AB (first ARB cycle) by dotted lines.

The Lankford parameters, normal and planar anisotropy differ very much for the starting materials. With increasing number of ARB cycles the value of r_{TD} decreases from 0.9 to 0.6, the value of r_{45° monotonously increases from 0.3 to 0.7, while the value of r_{RD} stays approximately constant at 0.5. Starting with a value of 0.5 after the first cycle the normal anisotropy reaches a plateau at 0.6 after 4 cycles, while the planar anisotropy decreases from 0.3 to a -0.1 until the 6th cycle and changes sign at the 4th cycle. The best deep drawing conditions are obtained for large normal anisotropy values and a planar anisotropy close to zero reducing thinning of the walls and minimizing earing, respectively. From Fig. 3 it can be concluded, that after 4 ARB cycles the most suitable conditions are achieved.

The results of the simulations are compared with experiment in Fig. 4. Even though the general trends of the simulations coincide with the experimental ones up to the 6th cycle, the absolute values can be quite different, especially for r_{RD} . Generally the simulations overestimate the experimental values, especially for r_{RD} . An increase of the strain-rate sensitivity index decreases the simulated values of the Lankford parameters. A similar effect is observed for decreasing activity of non-octahedral slip. Thus, the best simulation results are obtained for high strain-rate sensitivity and with only (111)<110> slip but r_{RD} still is about 2 times higher. Obviously, qualitative simulation of plastic anisotropy of such heterogeneous sheets cannot be satisfactorily simulated by using global textures. In [5], the same measurements and simulations were performed for aluminium produced by

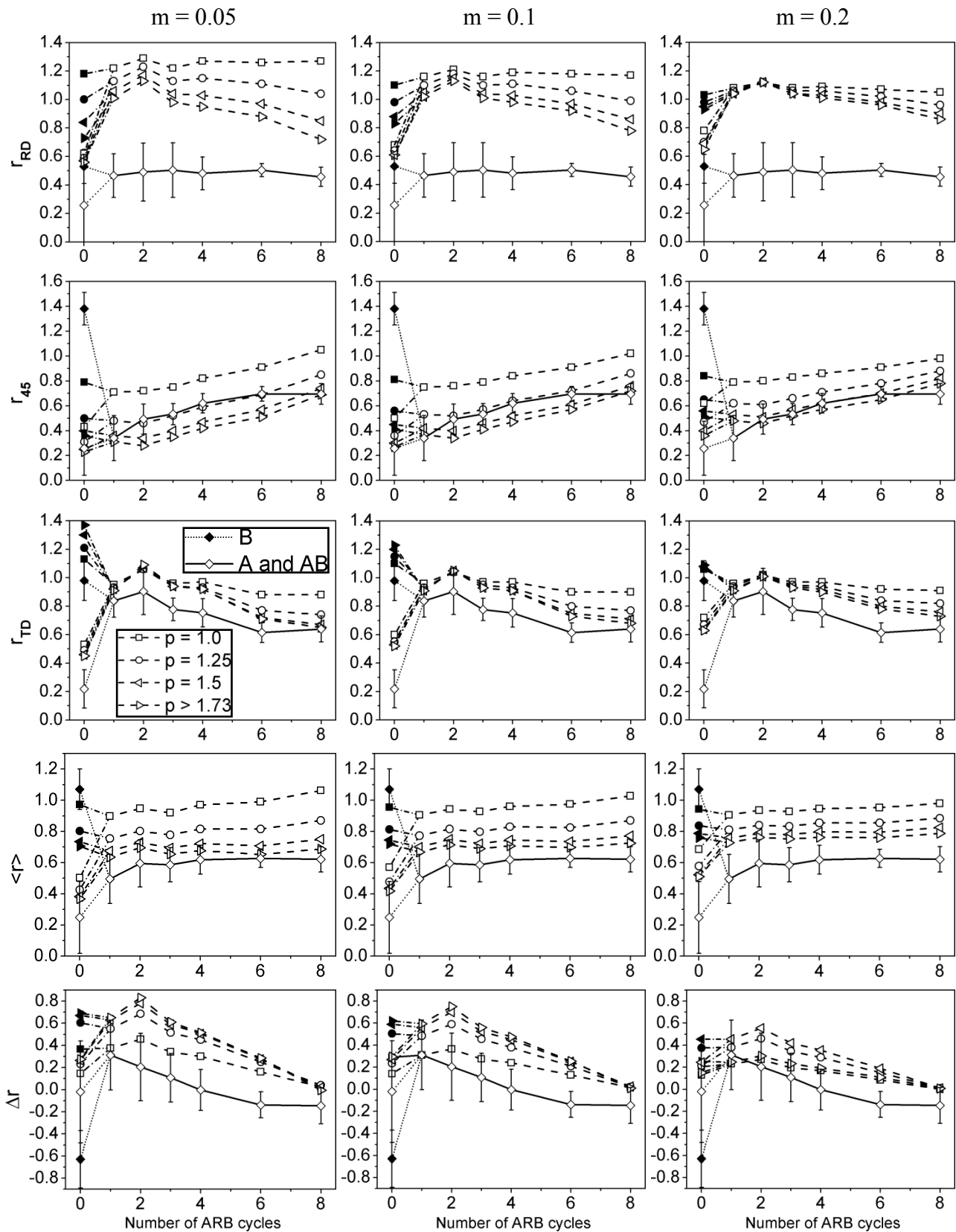


Fig. 4: Measured (solid lines) and simulated (dashed lines) Lankford parameter for different tensile directions, the normal ($\langle r \rangle$) and the planar (Δr) anisotropy for varying strain rate sensitivity m and different contribution of non-octahedral slip p as a function of the number of applied ARB cycles.

ARB of single B material. There, the results of the simulations are closer to those from experiment, especially for the initial material and after 8 cycles. The deviations for cycles in between were attributed to the texture heterogeneities, especially to the shear texture near to the surface. The highest deviations in [5] were observed at r_{45° and justified by the fact that the simulated r_{45° was about the same for a texture composed by the copper component and a texture by both rotated cube and copper component. In the present work the global textures do not show any noteworthy rotated cube component up to 6 cycles. However, in contrast to [5], now there is a dominant cube component localized in the recrystallized A layers. Considering the cube component crystallographically equivalent to the rotated cube rotated by 45° around ND, this may explain why the simulated Lankford parameters are strongly overestimated in r_{TD} and particularly r_{RD} . An additional difference is the discrete through-thickness distribution which is not comparable with a continuous gradient of the rotated cube component from surface to the middle of the sheet. Furthermore, the different hardness of the materials is not taken into account. It is understandable, that the deformation of the high purity aluminium layers requires less energy than that of the commercial purity ones. One possible approach to take this into account in the model may be achieved by weighting of the textures of the different materials. However this requires precise data on the local texture in each layer in order to get an exact separation of the global texture.

Summary

In this study it was demonstrated that laminates of different pure aluminium can be produced by ARB. In the high purity layers discontinuous recrystallization occurs, while the commercial purity layers form an ultrafine-grained structure by continuous recrystallization. The global texture and the mechanical anisotropy change with increasing number of ARB cycles. The viscoplastic polycrystal self-consistent model with the global texture as input predicts the trends of the changes of the plastic anisotropy. However the absolute values are not reproduced accurately enough. It is suggested that the special distribution of the texture and the different hardness of the layers has to be taken into account.

Acknowledgments

This work has been supported by the European Union and the Free State of Saxony in the framework of the European centre for emerging materials and processes (ECEMP), contract no. 13795/2379. B. Beausir is grateful to the Alexander von Humboldt Foundation for his research fellowship.

References

- [1] Y. Saito, N. Tsuji, H. Utsunomiya, T. Sakai, R.G. Hong, *Scripta Mater.* 39 (1998) 1221.
- [2] N. Tsuji, Y. Saito, H. Utsunomiya, S. Tanigawa, *Scripta Mater.* 40 (1999) 795.
- [3] H.W. Höppel, J. May, M. Göken, *Adv. Eng. Mater.* 6 (2004) 781.
- [4] M. Eizadjou, A. Kazemi Talachi, H. Danesh Manesh, H. Shakur Shahabi, K. Janghorban, *Composites Sci. Technol.* 68 (2008) 2003.
- [5] B. Beausir, J. Scharnweber, J. Jaschinski, H.-G. Brokmeier, C.-G. Oertel, W. Skrotzki, *Mater. Sci. Eng. A* 527 (2010) 3271.
- [6] R.A. Lebensohn, C.N. Tomé, *Acta Metall. Mater.* 41 (1993) 2611.
- [7] W. Truszkowski, J. Król, B. Major, *Met. Mat. Trans. A13* (1982) 665.
- [8] S. Gourdet, F. Montheillet, *Acta Mater.* 51 (2003) 2685.
- [9] M.Z. Quadir, O. Al-Buhamad, L. Bassman, M. Ferry, *Acta Mater.* 55 (2007) 5438.
- [10] M.E. Kassner, H.J. McQueen, J. Pollard, E. Evangelista, E. Cerri, *Scripta Metall. Mater.* 31 (1994) 1331.
- [11] G. Wassermann, *Texturen metallischer Werkstoffe*, 2nd ed., Springer Verlag, Berlin 1962.

Textures of Materials - ICOTOM 16

10.4028/www.scientific.net/MSF.702-703

Mechanical Anisotropy of Aluminium Laminates Produced by ARB

10.4028/www.scientific.net/MSF.702-703.151